iJournals: International Journal of Software & Hardware Research in Engineering
ISSN:2347-4890, ijournals.in/ijshre
Volume 13 Issue 4, April 2025

Biological Safety Cabinet Performance Study

Author: Chuang Zhang

Affiliation: North China Electric Power University, China

E-mail: 1415206632@qq.com

DOI: 10.26821/IJSHRE.13.04.2025.130305

ABSTRACT

Biosafety has become increasingly critical in the context of emerging infectious diseases and bioterrorism threats. Biosafety laboratories (BSLs) play a pivotal role in biomedical research and clinical diagnostics by providing controlled environments for handling pathogenic agents. Central to their containment systems are biosafety cabinets (BSCs), which serve as primary barriers against bioaerosol transmission through integrated directional airflow and HEPA filtration technologies. This study investigates the performance of biosafety cabinets (BSCs) under varying operational conditions, including temperature, air velocity, personnel activity, and aerosol release concentration. The research focuses on analyzing three key metrics: the sash leakage factor (SLF), protection factor (PF), and cabinet leakage factor (BLF). Numerical simulations and experimental validation were conducted in a BSL-2 Enhanced laboratory using Serratia marcescens as a tracer. Results show that lower temperatures (20°C) significantly enhance BSC performance, reducing SLF by 21.6% and BLF by 27.6% while increasing PF by 97.6% compared to high-temperature conditions (28°C). Optimal air velocity (0.5 m/s) minimizes SLF and BLF, with a 18.4% reduction in leakage risk. Personnel activities, particularly arm movements, drastically degrade performance, increasing SLF by 125% and reducing PF by 86%. Higher aerosol concentrations (1×10^{-5} CFU/mL) elevate SLF by 293.8% and BLF by 290.9%, indicating a critical threshold for safe operations. These findings provide actionable insights for optimizing BSC performance and laboratory biosafety protocols.

Keywords : Biosafety cabinet; Performance metrics; Temperature impact; Air velocity optimization; Personnel activity; Aerosol concentration; Laboratory safety; CFD simulation; Bioaerosol transmission.

1. INTRODUCTION

Infectious diseases are one of the leading causes of human death and disability worldwide, posing a major challenge to the progress and development of human society. According to statistics, the number of deaths due to infectious diseases is as high as 15 million per year globally [1]. Since entering the 21st century, frequent outbreaks of emerging infectious diseases have brought great losses to the human society, such as the epidemics of respiratory diseases such as Severe Acute Respiratory Syndrome (SARS), Middle East Respiratory Syndrome (MERS), tuberculosis (TB), and some novel infections (EIs) [2-6]. A biosafety laboratory is an important place for medical testing and scientific research, and plays a key role in responding to public health emergencies. It provides a relatively safe experimental environment for experimenters and is mainly used to carry out research work related to biological factors, which is of great significance to national security and

even global public health security. However, biosafety laboratories themselves have potential biosafety risks, and incidents of Laboratory-Acquired Infections (LAIs) have occurred from time to time [7-9].

In the study of aerosol generation and diffusion, Pottage et al. experimentally found that the titer and volume of spore suspensions and improper use of equipment are the key factors for aerosol generation [10].Feng explored the containment control of aerosols in biosafety laboratories from the perspective of mechanical engineering, and pointed out that reasonable air distribution strategies, stable pressure gradients, and the design of buffer chambers are important means to reduce the risk of aerosol exposure [11,12]. important means to reduce the risk of aerosol exposure [13]. In addition, optimization of equipment layout can improve room airflow organization and reduce particulate deposition on equipment and wall surfaces [14,15].

With the development of computational fluid dynamics (CFD) technology, its application in bioaerosol diffusion simulation has become more and more widespread.Yu et al. first applied CFD to virus diffusion simulation and verified its accuracy experimentally [16,17].Liu et al. combined CFD with orthogonal experimental design (OED) to analyze the effects of the contaminant source location, ventilation form, and the number of air change chambers (ACHs) on ventilation performance [18].Wang et al. investigated the spatial distribution and deposition characteristics of aerosols in a mobile biosafety level 4 (BSL-4) laboratory based on air-aging and particle tracking techniques [19,20].Zhuang et al. identified the high concentration areas of aerosols and their removal effects in a BSL-3 laboratory through numerical simulation and experimental validation [21-24].

As the core equipment of laboratory biosafety protection, the research on the protection efficacy of biosafety cabinets has been the focus of attention of the international academic community. Foreign scholars have carried out systematic studies around airflow organization optimization, operation specifications and environmental disturbances.Ibrahim et al. (2017) found through CFD numerical simulation that optimization of deflector design can significantly reduce the vortex zone inside the biosafety cabinet and improve the efficiency of contaminant capture [25].Hinrichs et al. (2016) used PIV technology to quantitatively show that the rapid movement of personnel can exacerbate the airflow disturbance of the front window, which can be caused by the rapid movement of personnel [26,27]. movement can exacerbate the airflow disturbance in the front window, and it is recommended to set up an anti-disturbance buffer zone around the operation area [28].Held et al. (2019) confirmed through thermal imaging experiments that the heat source inside the cabinet can lead to stratification of airflow, which affects the filtration efficiency, and put forward the design guideline that the layout of the equipment needs to maintain a reasonable heat dissipation spacing [29].Parks et al. (2022) demonstrated through a cyclic test that the front window opening exceeding the standard can significantly increase the risk of Parks et al. (2022) demonstrated that excessive front window opening significantly increased the risk of aerosol leakage through cyclic testing, validating the importance of standardized operating procedures [30,31]. It is therefore necessary to investigate the performance of biosafety cabinets

In this study, an enhanced biosafety level 2 laboratory (BSL-2 Enhanced) was used as a research object to conduct a systematic study on its special

safety protection requirements. The performance study was conducted for the biosafety cabinets in the laboratory.

2. METHOD

2.1 Case description

The physical model for this study was derived from the P2+ laboratory at North China Power University (NCPU). The physical model of the indoor part of the laboratory was simplified and constructed using Space Claim 2022R1 software, and the experimental equipment appeared in the form of rectangular boxes. As shown in Fig. 3(a), the dimensions of the laboratory are 7.2 m (X) × 5.6 m (Y) × 2.5 m (Z). In order to represent the individual walls more accurately and succinctly, they are labeled as X-, X+, Y-, Y+, Z-, and Z+, respectively, according to the direction of the coordinates. The laboratory is equipped with two laboratory tables, two B2 type biological safety cabinets, one fume hood, two refrigerators, two incubators, one autoclave and one transfer window. The ventilation system has three 0.65 m x 0.65 m supply air outlets with an air velocity of 0.5 m/s and two 0.95 m x 0.65 m return air outlets to maintain a negative pressure of -15 Pa in the room. These parameters meet the general requirements for biosafety laboratories. An upward and downward airflow pattern is also a common design for this type of facility. Table 1 lists the dimensions of each piece of laboratory equipment. In order to accurately replicate the movements of the laboratory staff, three laboratory operators were introduced into the model, located in front of Lab Table 1, Lab Table 2, and BSC1. The height of each operator was set to 1.7 meters with a corresponding body surface area of 1.6 .

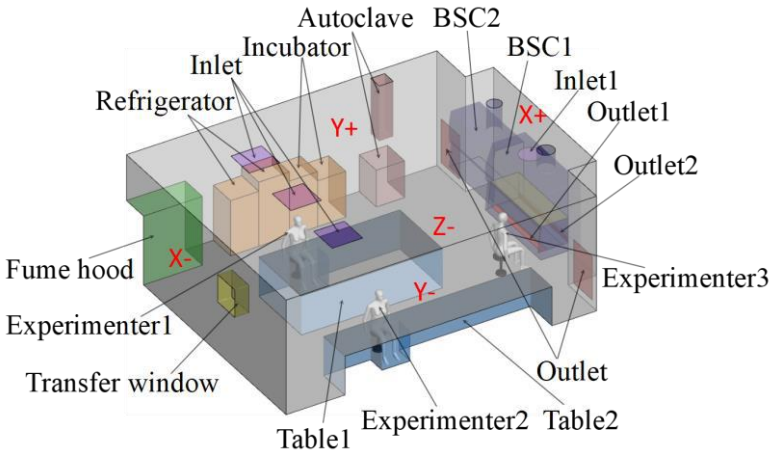

Figure 1. Physical model

2.2. Numerical model

range of turbulence models for indoor settings were examined and assessed by Zhang and colleagues in this study. The findings revealed that the RNG k-ε model performed exceptionally well in terms of accuracy, computational cost, and stability. Notably, the "augmented wall treatment" was adopted for characterizing turbulence in the vicinity of the wall. The governing equations can be expressed in a standard format.[32,33]

$$\partial(\rho\varphi)/\partial t+\nabla[(\rho\varphi\vec{u})=\nabla[(\Gamma_{\varphi}\nabla\varphi)+S_{\varphi}$$

Where ρ is the air density, $\vec{u}$ is the air velocity vector, φ is each of the three velocity components, Γ_{φ} is the effective diffusion coefficient of φ, and

S_φ is the source term.

The study employed the SIMPLE algorithm to separate pressure and velocity, and applied the second-order upwind scheme to discretize the convection and diffusion convection terms in the governing equation. The Boussinesq model was concurrently utilised to consider the buoyancy effect. Convergence was reached once the continuity residuals and scale velocity achieved a standard of 10-4, and the energy residuals reached 1×10^{-6}[34]

The Lagrangian method, specifically the discrete phase model, was adopted to track the particle motion. The effect of turbulence on particle diffusion was determined using the discrete random walk (DRW) model. The particle phase force consists of various forces, such as Brownian force, Basset force, Saffman lift force, virtual mass force, pressure gradient force and thermophoretic force. The particle motion, in particular, is primarily affected by thermophoretic and Safman forces [49]. The equation is presented below.

$$\frac{d\vec{u}_p}{dt}=\frac{18\mu}{\rho_p d_p^2}\frac{C_D\,\mathrm{Re}}{24}(\vec{\mu}+\vec{\mu}_p)+\frac{\vec{g}(\rho_p-\rho)}{\rho_p}+\vec{F}$$

where $\vec{u}$ and $\vec{u}_p$ are the velocity of airflow and particles; ρ and ρ_p are the density of airflow and particles, respectively; t is the time; $\vec{g}$ is gravitational acceleration; d_p is the diameter of the particles; Re is the particle Reynolds number; C_D is the drag coefficient; $\vec{F}$ is the additional forces acting on the particles.

3.RESULT

3.1. Dynamic migration of bioaerosols

Figure 2 shows the spatial and temporal distribution of bioaerosols at different moments for both Case1 and Case2. The different particle colors indicate the time points at which the particles are released. At 30s, the particles in both cases move with the downward airflow as well as the directional flow towards the corresponding exhaust ports, the particles in case1 reach BSC2 and the particles in case2 reach BSC1, and some of the particles migrate towards the interior of BSC1 due to the suction effect of the front window of BSC1. 120s the bioaerosol has been preliminarily dispersed, and the particles in case1 are mainly concentrated in the corners of the wall between X+ and Y+, which indicates that the concentration of bioaerosol is higher at the corners. case2 particles are mainly concentrated near the Y-plane, which is due to the fact that the experimental table is located at the edge of the laboratory, the directional flow is not obvious, and the airflow from the air supply outlet will hinder the particle discharging on the contrary. 210s when the bioaerosol particles generated in the first 30s were basically discharged, and only a small portion of them were suspended near the ceiling and the wall surface, the overall The overall trend is consistent with that of 120s. case2, due to the influence of vortex, part of the particles have migrated to the upstream of the laboratory, indicating that there is a certain risk of infection in the upstream of the laboratory. 300s, the bioaerosol has been released completely, and the concentration of particles reaches the maximum at this time, the distribution of particles in case1 has not changed significantly, mainly concentrated in the quarter of the area between X+ and Y+. The distribution range of particles in Case2 is wider, and there are distributions near both Y- and X+ surfaces, which indicates that the removal effect of release source 1 is better than

that of release source 2, and the cleaning effect of the airflow is more obvious.The bioaerosol particles are obviously reduced in 420s, and most of the particles in Case1 are those produced above 270s, while most of the particles in Case2 are those in the range of 180s-240s, which indicates that the removal efficiency of de-bioaerosolization of case1 is higher than that of case2.

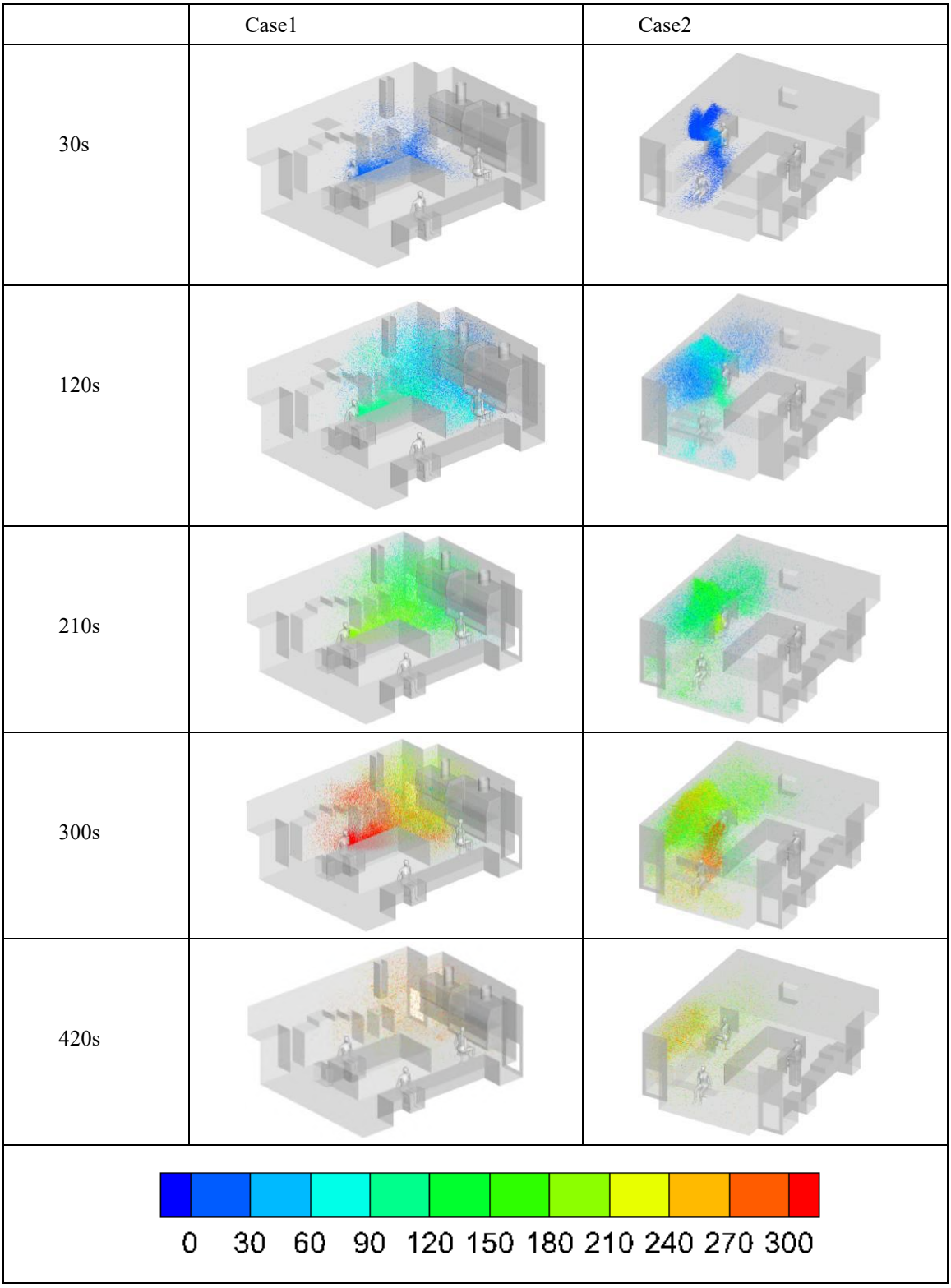

Fig. 2 Particle diffusion diagram

3.2 Biosafety Cabinet Flow Field Analysis

As the core protective equipment in a biosafety laboratory, the performance of a Biosafety Cabinet (BSC) is directly related to the safety of experimental personnel and the integrity of experimental samples. In this study, the BSC1 was operated in an open environment, as shown in Figure 3. The flow field of the biosafety cabinet is constructed by the inlet, the descending airflow, the inflow airflow, and the exhaust slots (Exhaust Slot 1 and Exhaust Slot 2). The inlet introduces external clean airflow, the downward airflow forms a vertical downward airflow barrier inside the cabinet, the inflow airflow forms a horizontal protective flow in the area of the front window, and the exhaust tanks assume the function of contaminant extraction. The air inlet, with a diameter of 0.45m, draws in a large volume of air from the room and provides a steady downward airflow of at least 0.3m/s. The exhaust chutes 1 and 2 have a diameter of 0.45m. The dimensions of exhaust chute 1 and exhaust chute 2 are 1.75m x 0.13m and 1.75m x 0.1m, respectively, with airflow velocities in excess of 0.7m/s. The type B2 biosafety cabinet (BSC) is a full-exhaust system that ensures that the exhaust airflow exceeds 1,449, and that the cabinet is negatively pressurized. The inflow airflow velocity at the front window is higher than 0.5 m/s, which meets the design criteria [45,46]. Figure 3 represents the velocity streamline cloud of this biosafety cabinet under normal operation, the descending airflow velocity in the operation area is 0.35±0.05 m/s, the inflow airflow velocity in the front window is 0.55±0.03 m/s, and the velocities of the dual exhaust slots are all greater than 0.7 m/s. The inflow airflow velocity in the front window is a key indicator of the protection performance of the BSC.

However, in the real experimental environment there will be many factors affecting the smooth and protective performance of BSC. Biosafety cabinets in the operation of infectious experimental materials, performance experiments can ensure its effective barrier pathogens and other harmful substances. Experiments to detect whether the filtration system, airflow pattern, etc. are working properly can prevent the leakage of infectious aerosols and spills generated during operation, avoiding the exposure of operators to hazardous biological factors and reducing the risk of laboratory infection . For example, if the High Efficiency Particulate Air (HEPA) filter of a biological safety cabinet is not working properly, it will leak contaminated air inside the cabinet, which will threaten the health of the operators. While good airflow patterns can prevent the spread of contaminants, abnormal airflow can lead to protection failure. According to previous studies, the main factors affecting the protective performance of biosafety cabinets include, ambient temperature, indoor air flow rate, laboratory personnel behavior, and the concentration of the release source. In this chapter, a specific experimental study of these four influencing factors is conducted.

The mean surface air velocity at the front window was measured to be 0.55 m/s, which was consistent with the numerical simulation results, with a velocity attenuation of 5-8% in the edge region.CFD simulation showed that the inflow air velocity was parabolically distributed along the height direction (Fig. 7a), with the maximum velocity occurring at 0.3 m from the bottom, which was in full compliance with the ISO 10648-1 standard of the 0.3-0.6 m/s range.

The velocity distribution of the descending airflow inside the BSC was uniform 0.35±0.05m/s, indicating that the airflow was well organized. However, at the edge of the operation area (within

0.1m from the front window), the velocity gradient reaches 0.15m/s/m, and there is a localized vortex (Ω=0.48), which may lead to aerosol retention. The dual exhaust tank design creates a negative pressure gradient (-15Pa to -25Pa) inside the cabinet, accelerating aerosol discharge. The exit velocity of the exhaust tank reaches 1.2 m/s, which is 23% higher than that of the single-tank design, effectively shortening the aerosol residence time (Fig. 10a).

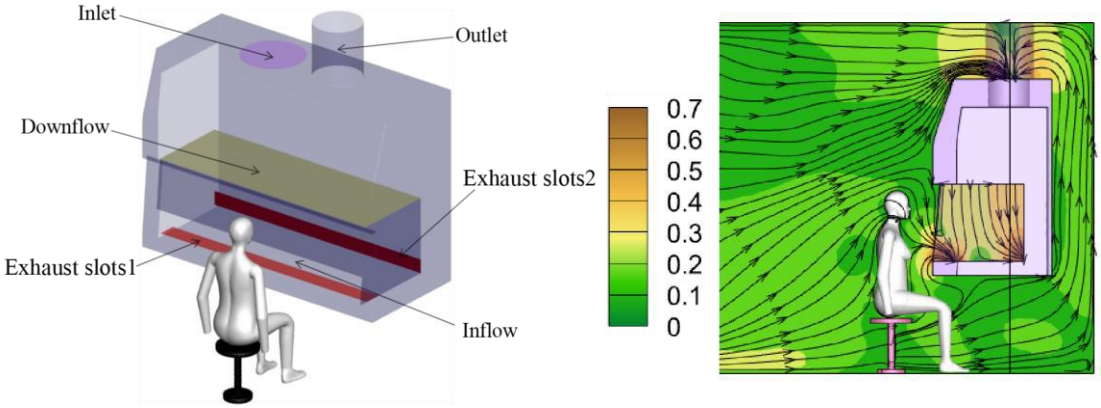

Fig. 3 BSC structure and flow field a) structure, b) flow field

3.3 Biosafety Cabinet Performance Experiment

Before the experiment, we used UV lamps and alcohol to sterilize the experimental environment in all aspects. After sterilization, the laboratory ventilation system was adjusted to maintain the air supply speed at 0.5 m/s, and the laboratory air conditioning system was adjusted to stabilize the indoor temperature at 24°C. The laboratory personnel were in front of the biological safety cabinet. The experimenter was in front of the biological safety cabinet. After the flow field of the room as well as the BSC was stabilized, a hot-wire anemometer (VELOCICALC 9545-A) was used to measure the airflow distribution inside and around the BSC. Three replicate measurements were performed for each measurement point. The results obtained were compared with the numerical simulation and the error was within 10%. Therefore the experiment is reasonable. The pre-configured Serratia marcescens stock solution was diluted to 1×CFU/mL. model bacteria release collection experiments were performed. The release sources as well as the measurement points are shown in Figure 6-2. Sampling points in the respiratory region were also included. Each experiment was 15 min, of which the release time was 5 min, using a bioaerosol generator (ZR-1050) in the center of the biosafety cabinet in the operating position for the aerosol release, the flow rate of the release was 28.3 L/min. the remaining 10 min for the bioaerosol migration to continue the study. An Anderson sampler was used in this experiment to collect from zero min until 15 min. Three replicate experiments were performed. After each experiment, the experimental environment was sterilized in all directions using UV lamps as well as alcohol to ensure that the experiment would not affect the next experiment. At the end of the experiment, the petri dishes from the three sampling sites were placed in an incubator for 24 hours to give constant temperature incubation. Then placed in the air for 10 hours. Pink circular colonies can be observed on the petri dishes. The data were counted and the concentration of bioaerosol was calculated according to Eq. In order to compare the performance of biological safety cabinets under

different working conditions more profoundly. The performance of the biosafety cabinet was evaluated using three indicators, which are front window leakage factor (SLF), protection factor (PF) and chamber leakage factor (BLF).

The Front Window Leakage Factor (SLF) represents the ratio between the leakage of contaminants through the front window opening and the concentration of contaminants inside the BSC, which provides a visual representation of the protective performance of the biosafety cabinet and indicates the amount of contaminant leakage. Protection Factor (PF) is the ratio of the concentration of pollutants in the exhaust of the BSC and the respiratory zone (height of 1.1m in the experimental personnel 3 around 1 place), this indicator can indicate the size of the probability of infection of the experimental personnel, the PF reflects the ability of the BSC to protect the experimental personnel. Box leakage factor (BLF) indicates the ratio of the concentration in the breathing region to the overall overall concentration of the laboratory as a whole. The formula is shown in Eq

where denotes the concentration of bioaerosol leaked from the front window of the BSC, denotes the concentration of bioaerosol inside the BSC, denotes the concentration of bioaerosol from the exhaust of the BSC, and denotes the concentration of bioaerosol in the respiratory region of the experimental personnel3. According to Chapter 3, Fig. The concentration of bioaerosol from the release source inside the biosafety cabinet under standard conditions can be calculated to be $1.28\times10^{-11}\,kg/m^3$, the concentration from the front window leakage to be $4.1\times10^{-14}\,kg/m^3$, and the concentration in the breathing zone to be $2.9\times10^{-15}\,kg/m^3$. The concentration of bioaerosol from the release source inside the biosafety cabinet under standard conditions can be calculated to be 2.9×. The values of SLF, PF, and BLF were calculated to be 3.2×10^{-3}, 7384, and 2.3×10^{-4} respectively, under standard conditions. According to previous studies, these three numerical indicators are within a reasonable range and comply with the design criteria of the biological safety cabinet.

The three experimental indicators are the key indicators describing the performance of the BSC. the lower the SLF and BLF, the higher the PF the better the protection performance of the biosafety cabinet. For example, Figure 6-3 shows the changes of the three performance indicators under four influencing factors.

Figure 3 shows the changes of the three indicators under the temperature conditions, SLF and BLF reached the lowest value at 20 ℃, respectively 0.0029 and 0.00021, while the PF reached the highest value of 8175. With the gradual increase in temperature, the SLF and BLF show a gradual increase in the trend, and the two trends are nearly the same. The SLF and BLF reached the highest values of 0.0037 and 0.00029, respectively, and the PF dropped to the lowest value of 4138 at 28°C. This trend indicates that the lower the temperature, the better the protection performance of the biological safety cabinet.

In terms of airflow, an increase in temperature leads to a decrease in air density. In the case of constant power of the biosafety cabinet fan, the actual air supply decreases. The reduction in air supply directly affects the organization of airflow inside the biological safety cabinet. Biosafety cabinets rely on a stable airflow to form an effective protective barrier. The descending airflow and the inflowing airflow from the front window work together to stop the leakage of bioaerosols. When the

air supply is insufficient, the stability and strength of the airflow is compromised, making it easier for bioaerosols to break through the protective barrier, thus increasing the risk of front window leakage. At the same time, higher temperatures increase the Brownian motion of microbial aerosols. Increased Brownian motion results in increased collision efficiency of microbial aerosol particles. This means that inside the biosafety cabinet, aerosol particles collide more frequently with each other and with the surfaces of other objects. This results in an elevated SLF. At the same time, the BLF is also elevated due to the decrease in the carrying and expelling capacity of the airflow for bioaerosols, which leads to a relative increase in the concentration of bioaerosols in the respiratory zone. Whereas PF is the ratio of the pollutant concentration in the exhaust port to the respiratory zone, an increase in the pollutant concentration in the respiratory zone and a relatively small change in the concentration in the exhaust port leads to a decrease in PF, i.e., a decrease in the ability of the biosafety cabinet to protect experimental personnel.

Figure 4 shows the changes of SLF, BLF and PF of the biological safety cabinet under different wind speed conditions. When the wind speed is 0.3 m/s, the SLF is 3.8×, the BLF is 0.0033, and the PF is 4008; as the wind speed increases to 0.5 m/s, the SLF decreases to0.0032, the BLF decreases to about .3×, and the PF rises to about 7200. When the wind speed is further increased to 0.7 m/s, the SLF rebounds to about 3.×, the BLF decreases to about 0.0012and the PF is 7635.

As the wind speed increases, the BLF and SLF decrease and the PF increases. This is due to the fact that the change in face air velocity directly affects the airflow barrier effect of the biosafety cabinet. When the wind speed is low (0.3 m/s), the ratio of the inlet flow rate at the front window to the air supply velocity in the room is relatively large, the airflow barrier is relatively weak, and the bioaerosol is easy to leak from the front window, resulting in a high SLF. As the wind speed increased to 0.5 m/s, the high air velocity enhanced the airflow barrier effect, effectively blocking the leakage of bioaerosols, resulting in a significant decrease in SLF. However, when the wind speed continues to increase to 0.7 m/s, the ratio of the inlet flow velocity to the indoor air supply velocity at the front window of the BSC decreases from 1.2 to 0.9, and the high flow velocity environment may weaken the airflow barrier effect of the BSC, and at the same time, the excessive wind speed (>0.7 m/s) triggers the turbulence (Re = 3500), which leads to localized vortices (Ω = 0.62), and in turn increases the risk of the leakage of the bioaerosol, making the SLF back up. For BLF, at lower wind speeds, the airflow has limited ability to carry bioaerosols, and the concentration of bioaerosols in the breathing zone is relatively high, and BLF is also high. With the increase of wind speed, the carrying and dilution ability of airflow for bioaerosols increased, the concentration of bioaerosols in the breathing zone decreased, and the BLF decreased. And PF as the ratio of pollutant concentration in the exhaust port and breathing zone, when the wind speed increases from 0.3m/s to 0.5m/s, the pollutant concentration in the exhaust port changes relatively little, and the pollutant concentration in the breathing zone decreases, resulting in the rise of PF, i.e., the protective ability of the biosafety cabinet for the experimental personnel is enhanced; however, the wind speed is further increased to 0.7m/s, due to the turbulence and other factors that lead to the pollutant concentration in the breathing zone to rise, PF decreases, and the protective ability of BLF is enhanced. rises, the PF

decreases, and the protection ability is weakened.

Figure 3 presents the changes of the three performance indicators of the biological safety cabinet under different activity states of the experimenters. When the experimental personnel waved their arms in front of the BSC, the SLF increased sharply to about 0.0072, the BLF increased to about 0.00038, and the PF decreased to 1034; when the experimental personnel moved horizontally in front of the BSC, the SLF was about 0.0043, the BLF was about 0.00031, and the PF was about 3123.

Personnel activities significantly affected the performance of the biosafety cabinet, mainly due to their interference with the internal airflow field. When the experimental personnel waved their arms, localized vortices were induced in the BSC operation area with a maximum reverse flow velocity of up to 0.15 m/s. Such localized vortices were sufficient to carry bioaerosols to penetrate the airflow barrier, which greatly increased the risk of leakage from the front window and resulted in a significant increase in SLF. At the same time, the localized vortex also makes the bioaerosol concentration in the breathing zone increase, BLF rises, and PF as the ratio of pollutant concentration in the exhaust port and the breathing zone, the pollutant concentration in the breathing zone increases dramatically, and the concentration in the exhaust port changes relatively little, resulting in a significant decrease in PF, and the ability of the biosafety cabinet to protect the experimental personnel is significantly weakened. When the experimenter moves laterally, although the degree of interference is slightly smaller relative to the swinging arm, but the same will produce a certain perturbation of the airflow field, making the SLF and BLF rise, PF decreases, affecting the protective performance of the biological safety cabinet.

Figure 4 reflects the change of performance indexes of the biological safety cabinet under different release source concentrations. When the release source concentration was 1×10^{-7}CFU/mL, the SLF was 0.0016, the BLF was 0.00011, and the PF was about 9800; when the release source concentration was increased to 1×10^{-6}CFU/mL, the SLF rose to 0.0032, the BLF was 0.00023 and the PF was 7384; when the releasing source concentration was further increased to 1×10^{-5}CFU/mL, SLF rose to 0.0063, BLF to approximately 0.00043, and PF to 2234.

Changes in release source concentrations directly affect the contaminant load inside the biosafety cabinet. When the release source concentration was low (1×10^{-7} CFU/mL), the bioaerosol concentration inside the biosafety cabinet was relatively low, and the concentration of bioaerosol leaking from the front window was also low, and the SLF was small. As the concentration of the release source increased, the concentration of bioaerosol inside the biosafety cabinet increased, and the concentration of bioaerosol leaking from the front window increased accordingly, and the relative proportion increased, resulting in a higher SLF. At the same time, the increase in the concentration of the release source causes the total amount of bioaerosol inside the cabinet to increase, and even if the biosafety cabinet tries its best to discharge the pollutants, the bioaerosol concentration in the respiratory zone will still increase relatively and the BLF is elevated. And PF as the ratio of pollutant concentration in the exhaust port and the respiratory zone, the increase of pollutant concentration in the respiratory zone and the relative change of the concentration in the exhaust port is small, which leads to the decrease of PF, i.e., the protection ability of the biological safety cabinet to the experimental personnel is weakened.

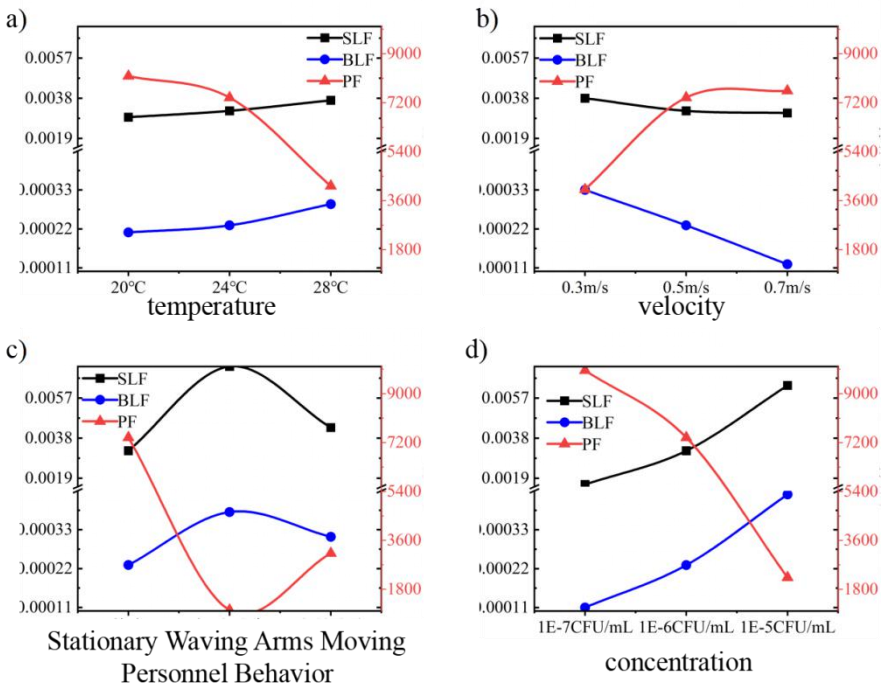

Fig. 4 Performance index of BSC with different factors

4. CONCLUSION

1. Temperature Impact: Lower temperatures (20°C) significantly enhance BSC performance, reducing the sash leakage factor (SLF) by 21.6% and cabinet leakage factor (BLF) by 27.6%, while increasing the protection factor (PF) by 97.6% compared to high-temperature conditions (28°C). This is attributed to improved airflow stability and reduced Brownian motion of bioaerosols.

2. Air Velocity Optimization: The optimal face velocity of 0.5 m/s minimizes SLF and BLF by 18.4%, achieving the highest PF (7200). Higher velocities (0.7 m/s) trigger turbulence and localized vortices, increasing leakage risks, whereas lower velocities (0.3 m/s) weaken airflow barriers, compromising protection.

3. Personnel Activity and Aerosol Concentration: Rapid arm movements near the BSC drastically degrade performance, increasing SLF by 125% and reducing PF by 86% due to airflow disturbances. High aerosol concentrations (1×10^{-5} CFU/mL) elevate SLF by 293.8% and BLF by 290.9%, surpassing safe operational thresholds. These findings emphasize strict adherence to standardized protocols and controlled environments for BSC safety.

5. REFERENCE

[1] Morens M D, Folkers K G, Fauci S A. The challenge of emerging and re-emerging infectious diseases . Nature: International weekly journal of science, 2004, 430.

[2] World Health Organization. Global tuberculosis report 2022[R]. Geneva: World Health Organization. 2022.

[3] Wu J, Leung K, Leung G. Nowcasting and forecasting the potential domestic and international spread of the 2019-nCoV outbreak originating in Wuhan, China: a modelling study. The Lancet. 2020.

[4] Ling, A. E . Editorial on Laboratory-Acquired Incidents in Taipei, Taiwan and Singapore following

the Outbreak of SARS Coronavirus. Applied Biosafety, 2007, 12(1):17-17.

[5] Ritger K , Black S , Weaver K , et al. Fatal laboratory-acquired infection with an attenuated Yersinia pestis Strain--Chicago, Illinois, 2009. . MMWR. Morbidity and mortality weekly report, 2011, 60(7):201-205.

[6] Traxler R M , Lehman M W , Bosserman E A , et al. A Literature Review of Laboratory-Acquired Brucellosis. Journal of Clinical Microbiology, 2013, 51(9):3055-3062.

[7] Azimi P, Stephens B. HVAC filtration for controlling infectious airborne disease transmission in indoor environments: Predicting risk reductions and operational costs. Building and Environment. 2013, 70: 150-160.

[8] Kojima K , Booth C M , Summermatter K , et al. Risk-based reboot for global lab biosafety. Science, 2018, 360(6386):260-262.

[9] Hinrichs T , Gragert S , Klein M . Biological Safety Cabinets: Simulation and Quantifying of Airflow Perturbation Caused by Personnel Activities. Applied Biosafety, 2016:1535676016635369.

[10] Yu I, Wong T, Chiu Y, et al. Temporal-spatial analysis of severe acute respiratory syndrome among hospital inpatients. Clinical Infectious Diseases. 2005, 40 (9): 1237-1243.

[11] Hathway E, Noakes C, Sleigh P, et al. CFD simulation of airborne pathogen transport due to human activities. Building and Environment. 2011, 46 (12) : 2500-2511.

[12] Stone L, Hastie D, Zigan S. Using a coupled CFD–DPM approach to predict particle settling in a horizontal air stream. Advanced Powder Technology. 2019, 30(4): 869-878.

[13] Zhang Y, Liu Y, Wang Y, et al. A comparative study of turbulence models for indoor airflow simulation. Building and Environment. 2010, 45(5):1109 - 1119.

[14] Liu W, Liu D, Gao N. CFD study on gaseous pollutant transmission characteristics under different ventilation strategies in a typical chemical laboratory. Building & Environment, 2017, 126(dec.):238 - 251.

[15] J. Wei, Y. Li, Enhanced spread of expiratory droplets by turbulence in a cough jet, Build. Environ. 93 (2015) 86–96.

[16] J. Ren, Y. Wang, Q. Liu, Y. Liu, Numerical Study of Three Ventilation Strategies in a prefabricated COVID-19 inpatient ward, Build. Environ. 188 (2021) 107467.

[17] Liu Z, Ma S, Cao G, et al. Distribution characteristics, growth, reproduction and transmission modes and control strategies for microbial contamination in HVAC systems: A literature review. Energy and Buildings. 2018, 177: 77-95.

[18] MARY L. LAUCKS, Aerosol Technology Properties, Behavior, and Measurement of Airborne Particles, J. Aerosol Sci. 31 (2000) 1121–1122.

[19] T.J. Chang, T.S. Hu, Transport mechanisms of airborne particulate matters in partitioned indoor environment, Build. Environ. 43 (2008) 886–895.

[20] B. Zhao, Y. Zhang, X. Li, X. Yang, D. Huang, Comparison of indoor aerosol particle concentration and deposition in different ventilated rooms by numerical method, Build. Environ. 39 (2004) 1–8.

[21] C. Wang, S. Holmberg, S. Sadrizadeh, Numerical study of temperature-controlled airflow in comparison with turbulent mixing and laminar airflow for operating room ventilation, Build. Environ. 144 (2018) 45–56.

[22] Li, M., Qi, J., Zhang, H., Huang, S., Li, L., Gao, D. Concentration and size distribution of bioaerosols in an outdoor environment in the Qingdao coastal region. Sci Total Environ , 2011, 409 (19), 3812–3819.

[23] Held K F , Thibeault R , Boudreau J . Heat Sources in a Biosafety Cabinet Compromise Experimental and User Protection. Applied Biosafety, 2019, 24(2):90-95.

[24] Parks S , Hookway H , Kojima K , et al. The Impact of Air Inflow and Interfering Factors on the Performance of Microbiological Safety Cabinets. Applied biosafety : journal of the American Biological Safety Association, 2022, 27(1):23-32.

[25] Zhu S, Demokritou P, Spengler J. Experimental and numerical investigation of micro-environmental conditions in public transportation buses. Building and Environment. 2010, 45 (10): 2077-2088.

[26] You R, Chen J, Lin C, et al. Investigating the impact of gaspers on cabin air quality in commercial airliners with a hybrid turbulence model. Building and Environment. 2017, 111: 110-122.

[27] Xu Y , Wang G , Xu M . Biohazard levels and biosafety protection for Mycobacterium tuberculosis strains with different virulence. Biosafety and health, 2020(3):7.

[28] Miki K. Particle motion determines the types of bioaerosol particles in the stratosphere. International Journal of Astrobiology, 2023, 22(3):205-215.

[29] Liu Z，Lv J，Zhang Z, et al. Three Experimental Common High-Risk Procedures: Emission Characteristics Identification and Source Intensity Estimation in Biosafety Laboratory. International Journal of Environmental Research and Public Health, (2023) 03-02.Harding A,

[30] Celik I B, Ghia U, Roache P J, et al. Procedure for estimation and reporting of uncertainty due to truncation error in CFD applications. Journal of Fluids Engineering, 2008, 130(7):078001.

[31] Azimi P, Stephens B. HVAC filtration for controlling infectious airborne disease transmission in indoor environments: Predicting risk reductions and operational costs. Building and Environment. 2013, 70:150 - 160.

[32] Qian H, Li Y, Nielsen P, et al. Spatial distribution of infection risk of SARS transmission in a hospital ward. Building and Environment. 2009, 44 (8): 1651-1658.

[33] Su W, Yang B, Melikov A, et al. Infection probability under different air distribution patterns. Building and environment, 2022(Jan. Pt. B):207.

[34] Tang S, Mao Y, Jones RM, et al. Aerosol transmission of SARS-CoV-2? Evidence, prevention and control. Environ Int. 2020;144:106039.